



Metallomics

Interference of pH buffer with Pb²⁺-peripheral domain interactions: obstacle or opportunity?

Journal:	<i>Metallomics</i>
Manuscript ID	MT-COM-01-2020-000002.R1
Article Type:	Communication
Date Submitted by the Author:	29-Jan-2020
Complete List of Authors:	Katti, Sachin; Texas A&M University, Biochemistry and Biophysics Igumenova, Tatyana; Texas A&M University, Biochemistry and Biophysics

SCHOLARONE™
Manuscripts

1
2
3
4
5
6
7
8
9
10
11
12
13
14
15
16
17
18
19
20
21
22
23
24
25
26
27
28
29
30
31
32
33
34
35
36
37
38
39
40
41
42
43
44
45
46
47
48
49
50
51
52
53
54
55
56
57
58
59
60

**Interference of pH buffer with Pb²⁺-peripheral domain interactions: obstacle
or opportunity?**

*Sachin Katti and Tatyana I. Igumenova**

Department of Biochemistry and Biophysics, Texas A&M University, 300 Olsen Boulevard,
College Station, TX 77843, United States

Corresponding Author

*tigumenova@tamu.edu

ABSTRACT

Pb²⁺ is a xenobiotic metal ion that competes for Ca²⁺-binding sites in proteins. Using the peripheral Ca²⁺-sensing domains of Syt1, we show that the chelating pH buffer Bis-Tris enables identification and functional characterization of high-affinity Pb²⁺ sites that are likely to be targeted by bioavailable Pb²⁺.

Significance to Metalloomics

Syt1, a key regulator of Ca²⁺-evoked neurotransmitter release, is a putative molecular target of Pb²⁺. We demonstrate that the use of a chelating pH buffer Bis-Tris enables identification of Ca²⁺-binding sites that would be most susceptible to Pb²⁺ attack in the cellular environment. In addition, experiments conducted in Bis-Tris revealed the differences between the membrane-binding responses of two Ca²⁺-sensing domains of Syt1, C2A and C2B. This work advances the understanding of how Pb²⁺ interacts with multipartite Ca²⁺-binding sites, and illustrates that conducting the experiments under both chelating and non-chelating conditions could provide valuable insight into the mechanism of C2-domain containing proteins.

1
2
3 Lead (Pb^{2+}) is a xenobiotic heavy metal ion that shows acute as well as chronic systemic
4 toxicity in the human body.¹ No extent of Pb^{2+} exposure is considered “safe”, and if undetected,
5 can cause irreversible neurological damage in young children.^{2,3} Among several proposed
6 modes of Pb^{2+} toxicity, the ability to mimic Ca^{2+} is particularly alarming, as it highlights the
7 vulnerability of ubiquitous, multi-site Ca^{2+} -binding proteins towards Pb^{2+} attack.⁴ Identification
8 of physiologically relevant Pb^{2+} -binding sites on these proteins is challenging because Pb^{2+}
9 interactions can be both specific as well as opportunistic, and often exhibit affinities higher than
10 those of native metal ions.⁵ Synaptotagmin 1 (Syt1), a key regulator of Ca^{2+} -evoked
11 neurotransmitters release⁶ and putative molecular target of Pb^{2+} ,⁷ provides a remarkable example
12 of this challenge. In the non-chelating environment such as MES buffer, four out of total five
13 Ca^{2+} -coordinating sites on the tandem C2 domains of Syt1 (C2A and C2B, **Fig. 1A**) bind Pb^{2+}
14 with affinities higher than Ca^{2+} .⁸ Site 1 on each domain exhibits sub-micromolar Pb^{2+} affinity,
15 while Site 2 is substantially weaker in comparison (**Fig. 1A, table**).

16
17 Here, we demonstrate, using the C2 domains of Syt1 as a paradigm, an approach that uses
18 a pH buffering agent and Pb^{2+} chelator, Bis-Tris, to selectively probe high-affinity Pb^{2+} sites and
19 determine their specific functional roles. Bis-Tris has five hydroxyl groups and one tertiary
20 amine group (**Fig. 1B**), all of which could potentially serve as ligands for a wide array of
21 divalent metal ions.⁹ While the challenges of using chelating pH buffers for metal ion-binding
22 studies are known,¹⁰ Bis-Tris was our chelator of choice because, compared to other strong
23 chelating agents such as EDTA, it forms weaker yet stable complexes with Pb^{2+} .⁹ In addition,
24 Bis-Tris is a highly adaptable chelator in that the number of its functional groups engaged in
25 metal-ion coordination can vary depending on the presence of competing ligands donated, e.g.,
26 by proteins, lipids, or other small molecules. We reasoned that due to these properties, Bis-Tris
27 would be a suitable mimic of a chelating physiological environment. In this work, we show that
28 not only the use of Bis-Tris enables discrimination between high- and low-affinity Pb^{2+} sites, it
29 also provides mechanistic information on the metal-ion dependent association of C2 domains
30 with anionic membranes. We therefore argue that a judicious use of chelating pH buffers in
31 metal-binding studies could provide a valuable insight into the mechanisms of metallosensory
32 proteins.

33
34
35
36
37
38
39
40
41
42
43
44
45
46
47
48
49
50
51
52
53
54
55
56
57
58
59
60

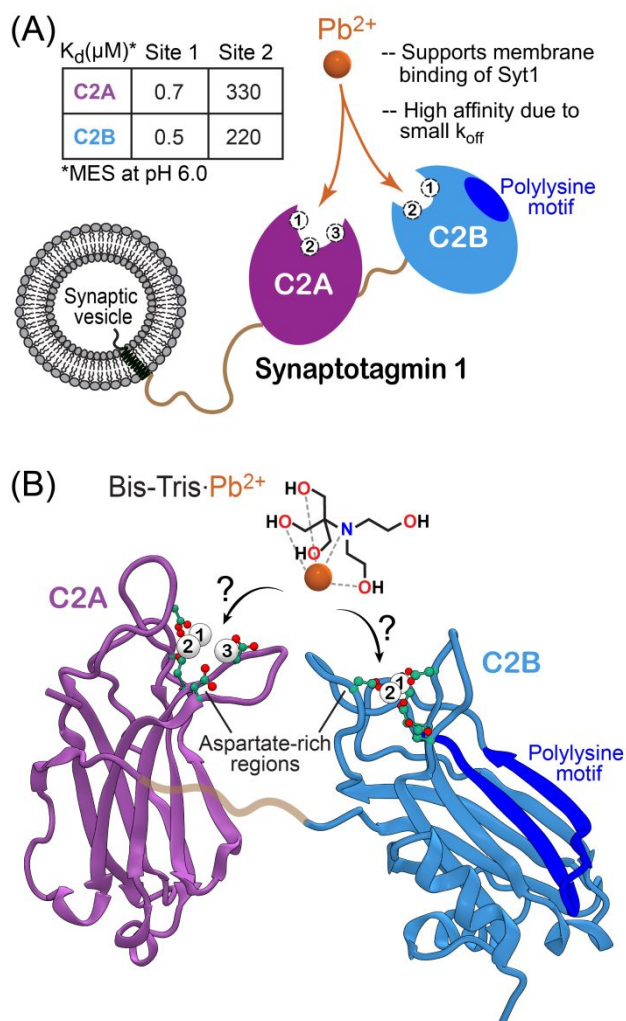


Figure 1. C2 domains of Syt1 interact with Pb^{2+} ions through the aspartate-rich loop regions.

(A) Schematic representation of Syt1, a neuronal transmembrane protein and its cytosolic C2 domains, C2A and C2B. Ca^{2+} -binding sites are labeled individually in each C2 domain. The affinities of Pb^{2+} to Sites 1 and 2 measured in MES buffer at pH 6.0⁸ are given in the table. The identities of residues that coordinate Pb^{2+} ion at Site 1 are given in **Table S1** of the SI. Pb^{2+} and Ca^{2+} do not appreciably bind to Site 3 under these conditions. (B) 3D structures of C2A (1BYN) and C2B (1UOW) domains showing the location of the Ca^{2+} -binding aspartate-rich sites within the apical loop regions. Also shown is the schematic representation of the Pb^{2+} complex with Bis-Tris. The exact coordination geometry of Pb^{2+} in the Bis-Tris complex is unknown.

To determine which of the five metal-binding sites of Syt1 are populated by Pb^{2+} in Bis-Tris, we conducted NMR-detected Pb^{2+} -binding experiments on the individual C2 domains, C2A and C2B. Solution NMR spectroscopy is best suited for this purpose because it enables clear identification of metal-ion binding sites with a wide range of affinities, as demonstrated previously for the C2 domains of Syt1 and protein kinase C (PKC).^{8,11} The information about protein-metal ion interactions is obtained by collecting 2D ^{15}N - ^1H hetero-nuclear single-quantum

1
2
3 coherence (HSQC) spectra of the uniformly ^{15}N -enriched ($[\text{U-}^{15}\text{N}]$) C2 domains, in the presence
4 of different concentrations of metal ions. Binding of a metal ion alters the electronic
5 environment of the backbone amide N-H_N groups that are proximal to the binding site, which
6 results in chemical shift changes of the $^1\text{H}_\text{N}$ and ^{15}N nuclei. Given the tendency of certain
7 buffering agents to interact with proteins,¹² prior to Pb^{2+} addition, we compared the metal-free
8 NMR spectra of the C2 domains in Bis-Tris and MES buffers. For C2A, the spectra in MES and
9 Bis-Tris were identical (**Fig. S1A**). For C2B, a subset of N-H_N resonances showed small
10 variations in their chemical shifts as well as intensities (**Fig. S1B**), indicating possible weak
11 interactions with one of these buffering agents. Because of the highly basic nature of C2B and
12 its propensity to interact with polyanionic molecules,¹³ the weakly interacting buffer is likely to
13 be MES.
14

15
16
17
18
19
20
21
22 Upon addition of Pb^{2+} to the C2A domain at a molar ratio of 2:1 ($\text{C2A}:\text{Pb}^{2+}$), we
23 observed an appearance of a subset of N-H_N cross-peaks that belong to the Pb^{2+} -complexed
24 protein species (top inset of **Fig. 2A**, cyan). Adding more Pb^{2+} to achieve a 1:1 molar ratio
25 results in the formation of a single protein species, the $\text{C2A}\cdot\text{Pb1}$ complex (**Fig. 2A** and top inset,
26 blue), where Pb^{2+} is bound to Site 1. This behavior is identical to that in the non-chelating MES
27 buffer,⁸ suggesting that Bis-Tris does not interfere with Pb^{2+} binding to Site 1 of the C2A domain
28 and full saturation of this site can be achieved at a stoichiometric ratio of protein to Pb^{2+} .
29

30
31
32
33
34 We found however that addition of more Pb^{2+} , with the objective to saturate Site 2 of the
35 C2A domain, did not produce a drastic change in the N-H_N cross-peak chemical shifts (**Fig. 2B**)
36 that we previously observed in MES.⁸ The Pb^{2+} binding event is in the “fast” exchange regime
37 on the NMR chemical shift timescale, where a single population-weighted cross-peak for a given
38 residue shows a smooth trajectory in response to increasing Pb^{2+} concentration. This behavior
39 enabled us to construct a binding curve by plotting the chemical shift perturbation Δ versus Pb^{2+}
40 concentration. The curve is linear, with no indication of reaching the cusp region even at 60-fold
41 excess of Pb^{2+} to protein (**Fig 2C**). For comparison, in MES, Pb^{2+} was able to saturate Site 2 of
42 the C2A domain at ~ 25 -fold excess to produce a K_d of $330\ \mu\text{M}$ (see **Fig. 1A**, table).⁸ We
43 observed the exact same pattern of Pb^{2+} interactions with C2B in Bis-Tris: complete population
44 of Site 1 at the stoichiometric protein-to- Pb^{2+} ratio, and extremely weak binding to Site 2 (**Fig.**
45 **S2**). We conclude that Bis-Tris does not affect Pb^{2+} binding to the high-affinity Site 1 but
46 inhibits the interactions of Pb^{2+} with Site 2 of both C2 domains of Syt1. This is in agreement
47
48
49
50
51
52
53
54
55
56
57
58
59
60

with the reported affinity of Pb^{2+} to Bis-Tris ($\log K_a=4.3$)⁹ that exceeds its affinity to Site 2 of the C2A domain. The affinity of Pb^{2+} to Site 3 of the C2A domain is too weak to be appreciably populated in either buffer.

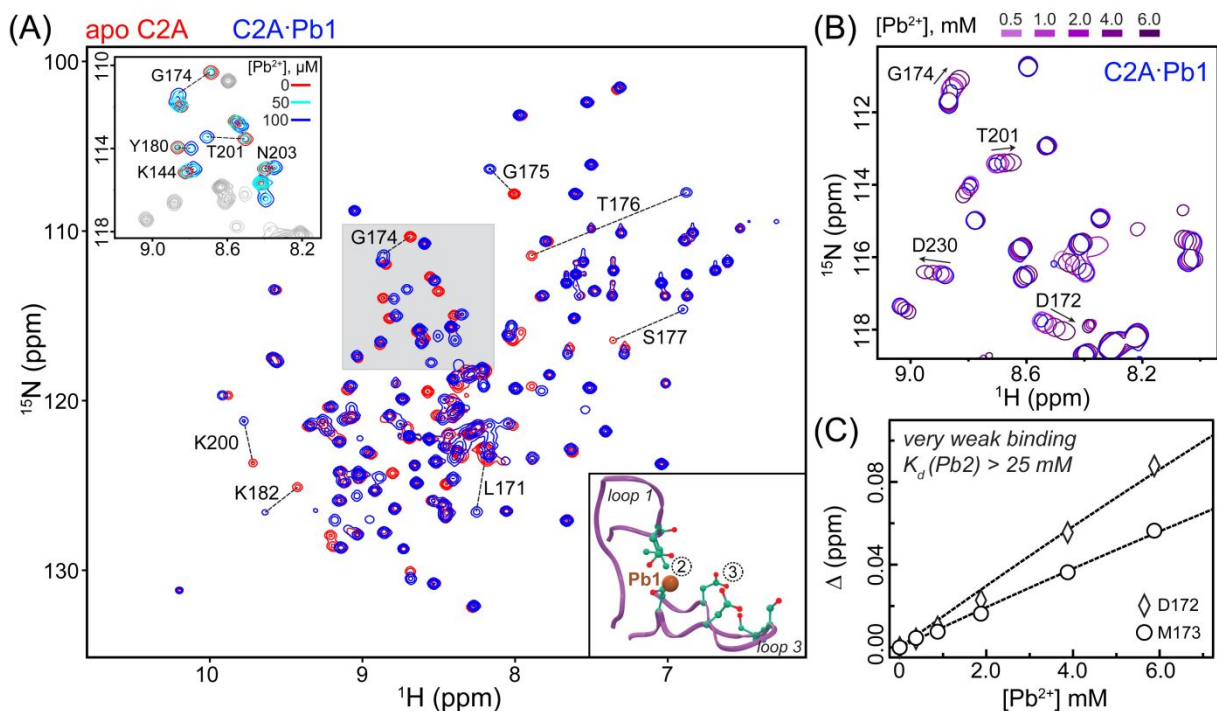


Figure 2. Bis-Tris inhibits Pb^{2+} binding to Site 2 but not Site 1 of the C2A domain. (A) Overlay of the ^{15}N - ^1H HSQC spectra in the absence (apo) and presence of stoichiometric Pb^{2+} (C2A: Pb^{2+} 1:1, 100 μM each) in 20 mM Bis-Tris buffer at pH 6.0. Residues showing response to population of Site 1 by Pb^{2+} are labeled. The spectra were collected at 25 $^\circ\text{C}$ on the Avance III NMR instrument (Bruker Biospin) operating at the magnetic field of 14.1 T and equipped with a cryogenically cooled probe. Top inset: expansion of the shaded spectral region with an additional Pb^{2+} concentration point (50 μM , C2A: Pb^{2+} 2:1, cyan) to illustrate the distinct chemical shifts of apo C2A and the C2A·Pb1 complex. Bottom inset: loop regions of the C2A domain showing the positions of Sites 1-3. (B) Overlay of the ^{15}N - ^1H HSQC expansions showing the chemical shift perturbations of several residues in the C2A·Pb1 complex due to Pb^{2+} binding to Site 2. (C) Chemical shift perturbations Δ (calculated as described in ref. 8) of two representative residues plotted as a function of Pb^{2+} concentration. The linear, non-saturatable profiles indicate that binding is extremely weak with a K_d of $>25 \text{ mM}$. The lines are to guide the eye.

1
2
3 We then asked if the Pb^{2+} dependent membrane-binding function of the C2 domains is
4 influenced by Bis-Tris. When Pb^{2+} populates high- as well as low-affinity sites, as is the case in
5 the MES buffer, both C2 domains interact readily with anionic membranes.⁸ However, when we
6 conducted the C2A-vesicle co-sedimentation experiments in Bis-Tris, we found that Pb^{2+} was
7 unable to support the membrane-binding function of the C2A domain. The fraction of the Pb^{2+} -
8 complexed protein bound to PtdSer-containing large unilamellar vesicles (LUVs) does not
9 exceed 5%, even under conditions of the 40-fold molar excess of Pb^{2+} over C2A (**Fig. 3A**). A
10 control experiment with the native metal ion, Ca^{2+} , produced a fractional population of the
11 membrane-bound species comparable to that observed in MES.⁸ Clearly, the effect of Bis-Tris is
12 specific to the Pb^{2+} -C2A-anionic membrane system. To ascertain that this finding is not
13 technique-dependent, we conducted FRET-detected protein-to-membrane binding experiments
14 shown schematically in **Fig. 3B**. In the presence of Ca^{2+} , the FRET curve of the C2A domain
15 represents a typical membrane binding response reported for the C2 domains (**Fig. 3C**).^{11, 14} In
16 contrast, we observed no Pb^{2+} -driven interactions of C2A with membranes in Bis-Tris, which is
17 fully consistent with the co-sedimentation data of **Fig. 3A**. We therefore conclude that Bis-Tris
18 interferes with the membrane-binding function of the Pb^{2+} -complexed C2A domain.
19
20
21
22
23
24
25
26
27
28
29
30

31 To understand the underlying cause of this behaviour, we considered two factors that are
32 essential for driving the C2A-membrane interactions:¹⁵ (1) the general “electrostatic shift” due to
33 metal-ion binding, which alters the charge of the intra-loop region from negative to positive; and
34 (2) the specific interactions of anionic phospholipid headgroups with the C2-complexed metal
35 ions (and potentially the basic residues of C2A surrounding the loop region). Our data indicate
36 that inhibition of Pb^{2+} interactions with Site 2 by Bis-Tris locks the C2A domain in the single
37 Pb^{2+} -bound state, and that the resulting electrostatic shift is insufficient for the C2A to engage in
38 high-affinity interactions with anionic membranes.
39
40
41
42
43
44
45
46
47
48
49
50
51
52
53
54
55
56
57
58
59
60

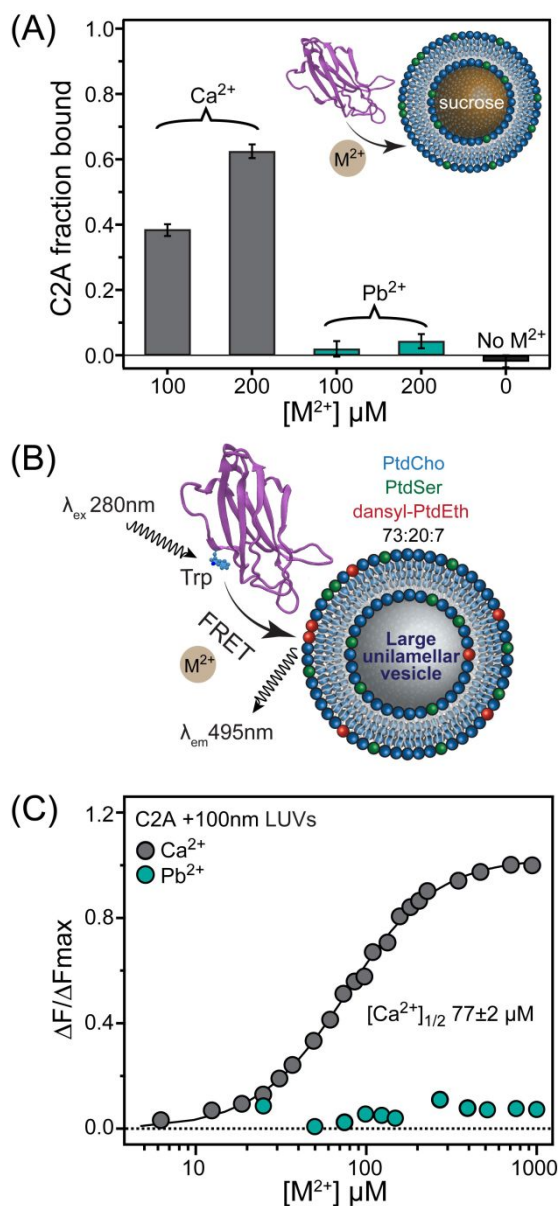


Figure 3. Pb²⁺-dependent membrane binding of C2A is abolished in the presence of Bis-Tris. (A) Fraction of C2A bound to sucrose-loaded LUVs in the presence of Ca²⁺ and Pb²⁺. The co-sedimentation experiments were conducted in 20 mM Bis-Tris at pH 7.0 and 150 mM KCl. The LUVs were 100 nm in diameter and consisted of PtdCho:PtdSer=80:20 (% molar). The C2A concentration was 5 μM . (B) Schematic representation of FRET-detected C2-membrane binding experiments. The resonance energy transfer takes place between native Trp residues and dansyl-PE fluorophore embedded into LUVs. (C) FRET-detected C2A-membrane binding curves plotted as a function of increasing M²⁺ (M=Ca, Pb) concentrations. The change in fluorescence intensity at 495 nm, ΔF , was normalized to the maximum change observed in Ca²⁺-dependent experiments, ΔF_{max} . Same buffer as for co-sedimentation experiments was used. The C2A concentration was 0.5 μM .

1
2
3 We next sought to investigate if specific interactions of the Pb^{2+} -complexed C2A domain
4 with PtdSer are influenced by Bis-Tris. PtdSer is the most abundant anionic lipid component of
5 the eukaryotic plasma membranes. It recruits metal ion-complexed C2 domains to membranes
6 by engaging in electrostatic interactions with the protein and forming specific coordination
7 bonds(s) with the protein-bound metal ion(s). In MES, the C2A·Pb1 complex prepared by
8 mixing stoichiometric amounts of C2A and Pb^{2+} associates weakly with PtdSer-containing
9 bicelles.¹⁶ The chemical exchange process between the C2A·Pb1-PtdSer ternary complex and
10 the C2A·Pb1 binary complexes occurs on the “fast-to-intermediate” NMR chemical shift
11 timescale. This produces a specific pattern of resonance intensity decrease in the NMR spectra
12 that predominantly affects the loop regions of the C2A domain. Here, we used a short-chain
13 PtdSer analogue, 1,2-dihexanoyl-*sn*-glycero-3-[phospho-L-serine] (DPS) to determine how Bis-
14 Tris influences the interactions of the C2A·Pb1 complex with PtdSer. In MES, addition of 5 mM
15 DPS to 100 μM [^{15}N enriched] C2A·Pb1 complex resulted in attenuation of the cross-peak
16 intensities. The attenuation was quantified as the ratio of the N-H_N cross-peak intensities in the
17 absence (I_0) and presence (I) of DPS. Consistent with previous data obtained using PtdSer
18 containing bicelles,¹⁶ residues that belong to the loop regions showed significant decrease in I/I_0
19 values, along with several residues in the polylysine region between loops 1 and 2 (**Fig. 4A**). In
20 contrast, the C2A·Pb1 complex in Bis-Tris showed little attenuation of signals that belong to the
21 loop regions (**Fig. 4B**). This is especially evident in the difference I/I_0 plot (**Fig. 4C**) that was
22 constructed by subtracting the data in (**B**) from the data in (**A**). We conclude that specific
23 interactions of the C2A·Pb1 complex with PtdSer, while clearly present in the non-chelating
24 MES buffer, are absent in the chelating Bis-Tris buffer. How does Bis-Tris inhibit the
25 interactions of the C2A·Pb1 complex with PtdSer? There are examples of crystal structures of
26 protein-metal ion complexes where Bis-Tris provides additional ligands to the protein-bound
27 metal ions.¹⁷⁻¹⁹ It is therefore plausible that Bis-Tris directly coordinates Pb1 and thereby
28 prevents Pb^{2+} to form coordination bonds with the oxygens of PtdSer. This scenario is
29 schematically shown in **Fig. 4D**.

30
31
32
33
34
35
36
37
38
39
40
41
42
43
44
45
46
47
48
49
50 In conclusion, Bis-Tris eliminates two factors that contribute to metal ion-driven C2A-
51 membrane interactions: the effect of general electrostatics, by inhibiting Pb^{2+} binding to Site 2;
52 and the effect of C2A·Pb1-PtdSer interactions, likely by completing the coordination sphere of
53 C2A-bound Pb1. These findings provide the following insight into the metal-ion dependent
54
55
56
57
58
59
60

1
2
3 membrane binding function of the C2 domains. C2 domains with partially occupied metal-ion
4 binding sites, through weak association with anionic membranes, are brought close to the polar
5 membrane region.^{16, 20} It is believed that the resulting proximity to anionic lipid moieties elicits
6 cooperative metal-ion binding to the remaining weaker sites by enhancing their affinities. This
7 mutual cooperativity enables the domain to perform its function at physiological concentrations
8 of Ca^{2+} .¹⁴ Our results support this mechanistic model: by interfering with the PtdSer interactions
9 of the C2A·Pb1 complex, Bis-Tris also precludes the cooperative enhancement of Site 2 affinity
10 towards Pb^{2+} . As a result, the domain stays locked in Pb1-bound state, unable to achieve
11 complete electrostatic shift required for membrane association.
12
13

14
15
16
17
18
19 When viewed from the perspective of Pb^{2+} toxicity, our data indicate that in the cellular
20 environment where Bis-Tris-like chelators and metabolites are abundant,²¹ the membrane
21 interactions of the C2A·Pb1 complex are unlikely to occur. Combined with our previous finding
22 that the presence of Pb^{2+} in Site 1 of C2 domains desensitizes them to further Ca^{2+} binding,^{8, 11}
23 the ability of Pb^{2+} -complexed C2A domain to interact with membranes is unlikely to be restored
24 or rescued at physiological Ca^{2+} concentrations.
25
26
27
28

29
30
31 The next step was to determine how Pb^{2+} -complexed C2B interacts with anionic
32 membranes in Bis-Tris. The C2B domain is significantly more basic than C2A due to the
33 presence of a distinct polylysine motif (see **Fig. 1B**), and additional positively charged residues,
34 Arg 398 and Arg 399, at the end opposite to the loop regions. Although the polylysine region is
35 located several Ångstroms away from the metal-ion binding loops, it plays a critical role in the
36 membrane association process.²²⁻²⁴ In particular, its interaction with the second messenger
37 PtdIns(4,5) P_2 dramatically increases the Ca^{2+} affinity to C2B, lowering the Ca^{2+} concentration
38 threshold required for the membrane association of this domain.²⁵ The underlying basis of this
39 cooperative effect is the change of the electrostatic potential of C2B, caused by the interactions
40 of its basic regions with anionic phospholipids. The cooperativity between anionic
41 phospholipids and divalent metal ions is mutual: binding of metal ions to the loop regions
42 enhances the interactions of C2B with phospholipids.
43
44
45
46
47
48
49
50
51
52
53
54
55
56
57
58
59
60

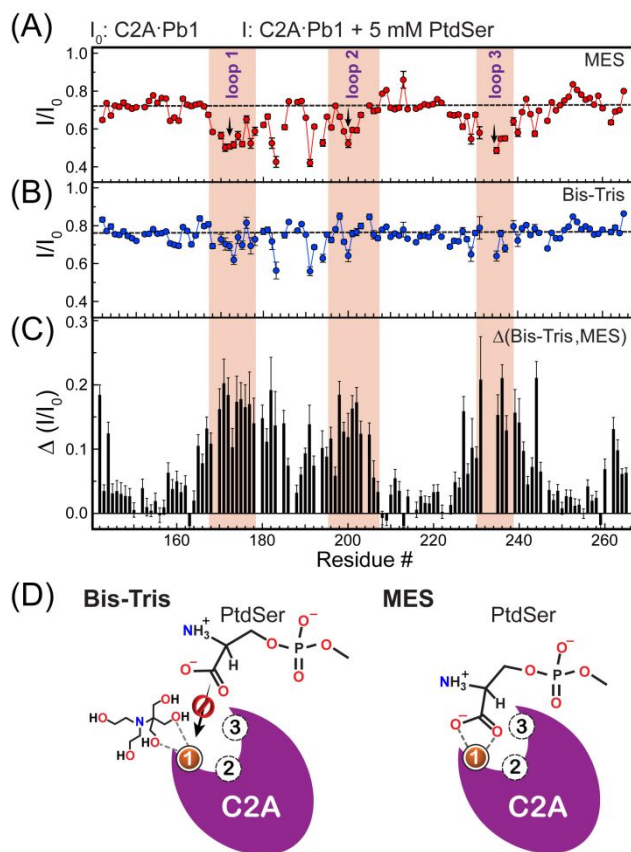


Figure 4. Pb^{2+} -complexed C2A domain does not appreciably interact with PtdSer in the presence of Bis-Tris. Attenuation of peak intensities in the C2A-Pb1 complex upon addition of 5 mM DPS, expressed as residue-specific I/I_0 ratios, where I and I_0 are the peak intensities in the presence and absence of PtdSer, respectively. The data were collected at pH 6.0 in 20 mM (A) MES and (B) Bis-Tris buffers. The errors in the intensity ratios were estimated using the r.m.s.d. of the base-plane noise in each of the collected spectrum. (C) The difference between I/I_0 ratios, demonstrating that the specific interaction of the C2A-Pb1 loops with PtdSer is present in the MES but not in the Bis-Tris buffers. (D) Schematic model showing how Bis-Tris can potentially interfere with C2A-Pb1-PtdSer interactions.

In stark contrast to C2A, Pb^{2+} -complexed C2B associates with LUVs in Bis-Tris (Fig. 5A, compare with Fig. 3A), with fractional population of the membrane-bound protein species comparable to that observed in presence of Ca^{2+} . The FRET experiments were carried out by titrating the PtdSer-containing LUVs into a solution containing C2B and excess Pb^{2+} , to minimize C2B-induced LUV clustering and associated increase in scattering.²⁶ The FRET results mirrored those of the co-sedimentation experiments. Pb^{2+} was almost as effective as Ca^{2+} in driving protein-membrane association, producing $[PtdSer]_{1/2}$ values of 3.4 μM compared to 2.8 μM , respectively (Fig. 5B). The two plausible explanations for this behaviour are: (1) the inherently basic nature of the C2B surface that enables membrane interactions in single Pb^{2+} -

1
2
3 bound state; and (2) the allosteric enhancement of C2B affinity to Pb^{2+} upon interactions of
4 PtdSer with basic regions of the protein.
5

6 To assess the relative contribution of these factors, we added DPS to the [$U\text{-}^{15}\text{N}$]
7 C2B·Pb1 complex (prepared by mixing stoichiometric amount of C2B and Pb^{2+}) and compared
8 the chemical shifts of the backbone amide groups between the NMR spectra of DPS-free and
9 DPS-containing samples of C2B·Pb1. We observed modest changes in the chemical shifts of the
10 C2B·Pb1 resonances that are located predominantly near the polylysine motif and the adjacent
11 “bottom” part of C2B (**Fig. 5C**), suggesting that these regions are the primary PtdSer interaction
12 sites. The nature of the C2B·Pb1-DPS interactions is electrostatic and is therefore expected to
13 produce large chemical shift changes if the protein is fully DPS-bound. The small values of
14 chemical shift perturbations suggest that the fractional population of the DPS-bound C2B·Pb1
15 species is small. Therefore, the inherently basic nature of C2B alone cannot explain the affinity
16 of Pb^{2+} -complexed C2B species to anionic membranes in Bis-Tris.
17
18
19
20
21
22
23
24

25 Next, we tested if the presence of PtdSer in solution enhances the affinity of C2B towards
26 Pb^{2+} to the extent that the domain acquires an ability to compete with Bis-Tris and bind the
27 second Pb^{2+} ion. Upon addition of 5-fold molar excess of Pb^{2+} to the C2B·Pb1 in the presence of
28 5 mM DPS, a new subset of cross-peaks appeared in the NMR spectrum (**Fig. 5D**, red spectrum).
29 This indicates the formation of new Pb^{2+} -bound species of the C2B domain that are in slow
30 exchange on the NMR chemical shift timescale with the C2B·Pb1 complex. The only possible
31 Pb^{2+} interaction site with the C2B domain is Site 2. Indeed, residues whose cross-peaks are
32 typically exchange-broadened in the C2B·Pb1 complex but only appear upon population of Site
33 2, G305 and D365, are detectable in the sample containing Pb^{2+} excess. For several residues,
34 more than two sets of resonances could be seen, reflecting the complex speciation of Pb^{2+} -bound
35 C2B in the presence of DPS. In the absence of PtdSer, the population of Site 2 in C2B by Pb^{2+} is
36 negligible even at 60-fold molar Pb^{2+} excess (**Fig. S2**). Therefore, we conclude that
37 neutralization of the polylysine region via interactions with PtdSer and, to generalize, anionic
38 phospholipids, is the dominant factor that enables the weaker Site 2 of C2B to successfully
39 compete with Bis-Tris for Pb^{2+} . The resulting acquisition of a full complement of Pb^{2+} ions by
40 the C2B domain, and the mutual cooperativity between the polylysine motif and metal-ion
41 binding loop regions drives the membrane association of C2B. This scenario is schematically
42
43
44
45
46
47
48
49
50
51
52
53
54
55
56
57
58
59
60

illustrated in **Fig. 5E**. In contrast to C2B, C2A showed barely any response to the addition of excess Pb^{2+} in the presence of 5 mM DPS (**Fig S3**).

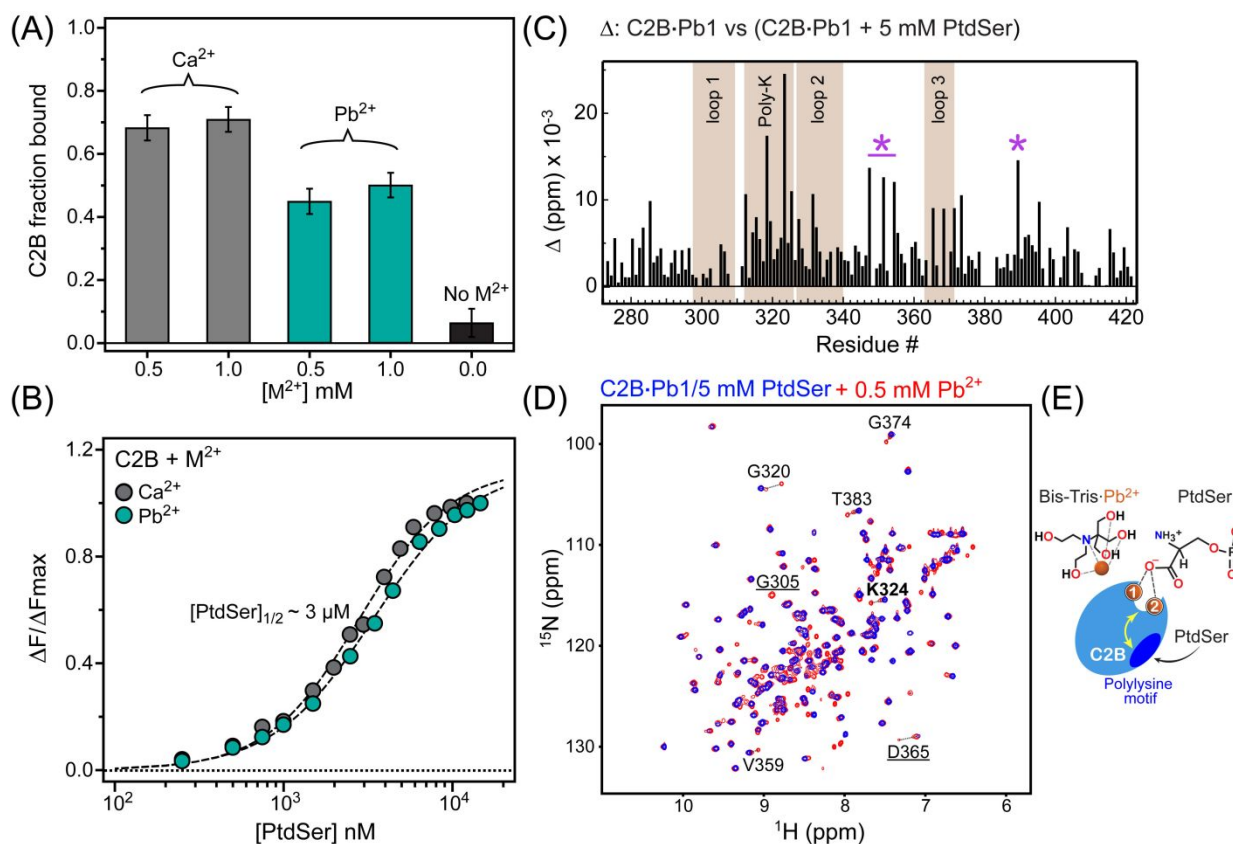


Figure 5. Pb^{2+} -dependent membrane binding of C2B persists in the presence of Bis-Tris. (A) Vesicle co-sedimentation experiments conducted in 20 mM Bis-Tris and 150 mM KCl at pH 7.0 show that in contrast to C2A, Pb^{2+} -complexed C2B associates with anionic membranes. The C2B concentration is 5 μM . (B) C2B-to-membrane binding curves plotted as normalized FRET efficiency versus accessible PtdSer concentration in LUVs. The concentrations of C2B and M^{2+} are 0.5 μM and 500 μM , respectively. Pb^{2+} is almost as effective as Ca^{2+} in driving membrane interactions. (C) Chemical shift perturbations Δ caused by addition of DPS (cmc \sim 12 mM) to the C2B-Pb1 complex are plotted as a function of primary structure. The polylysine motif and residues at the “bottom” of C2B, marked by asterisks, are the likely interaction sites based on the chemical shift data. (D) Overlay of the ^{15}N - ^1H HSQC spectra showing an additional set of cross-peaks that appears upon addition of 0.5 mM Pb^{2+} to the C2B-Pb1 complex in the presence of 5 mM DPS. The newly formed Pb^{2+} -bound C2B species are in slow exchange with the C2B-Pb1 species, as illustrated for residues G320, G374, T383, D365, and V359. The underlined residues G305 (loop 1) and D365 (loop 3) are broadened beyond detection in C2B-Pb1 but re-appear in the spectra upon Site 2 population by Pb^{2+} . K324, shown in boldface, is a residue that belongs to the polylysine motif. (E) A model that schematically illustrates how interactions of anionic phospholipids with the polylysine motif of C2B could cause cooperative enhancement in Pb^{2+} affinities for the metal-ion binding sites of the C2B domain. This effect would enable C2B to effectively compete with Bis-Tris for Pb^{2+} and acquire a full complement of Pb^{2+} ions needed for membrane interactions.

1
2
3 In full-length Syt1, the C2A and C2B domains are connected by a flexible 9-residue
4 linker and together form the full Ca^{2+} -sensing unit (**Fig. 1B**).²⁷ To determine how Pb^{2+} -driven
5 interactions of the C2AB fragment depend on the chelating properties of the environment, we
6 conducted FRET-detected protein-to-membrane binding experiments in MES and Bis-Tris (**Fig.**
7 **6A**). Due to the multivalent membrane binding mode of C2B²⁸ and the ability of the tandem C2
8 domains to interact with LUVs in “trans” mode with respect to each other,²⁹ the C2AB fragment
9 shows significant clustering of LUVs. The clustering thresholds are marked in red (**Fig. 6A**),
10 and correspond to the accessible PtdSer concentration upon exceeding which visible
11 precipitation of LUVs and concomitant decrease of FRET signal occur.
12
13
14
15
16
17
18

19 The most drastic difference between the binding curves of **Fig. 6A** is the overall decrease
20 of FRET efficiency in the Bis-Tris buffer: at 2.5 μM accessible PtdSer, the FRET efficiency is
21 ~3-fold lower than that in MES. This suggests that C2AB-membrane interactions are
22 significantly weakened in the presence of Bis-Tris. Based on the properties of individual
23 domains in Bis-Tris (**Figs. 3 and 5**), this behaviour is likely caused by the impairment of the C2A
24 membrane-binding function. This conclusion is further supported by the observation that the
25 clustering threshold in Bis-Tris requires more than twice the accessible PtdSer, 5.7 μM , than that
26 in MES.
27
28
29
30
31
32

33 In addition to providing mechanistic information about the determinants of C2-membrane
34 association, our data on the isolated domains and the C2AB fragment in Bis-Tris led us to
35 propose a model of how Pb^{2+} would interact with Syt1 under the chelating conditions of the
36 cellular milieu (**Fig. 6B**). Due to the competition with the physiological chelators such as
37 glutathione and metallothionein,^{21, 30} only high-affinity Pb^{2+} binding sites of Syt1 will be
38 populated, i.e. Site 1 of each C2 domain. Upon population of Site 1 by Pb^{2+} , C2B domain will
39 interact with anionic lipids of the presynaptic membranes, PtdIns(4,5) P_2 and PtdSer,¹⁶ via the
40 polylysine motif; due to the positive cooperativity, the affinity of C2B to divalent metal ions will
41 be enhanced. As we demonstrated previously,^{8, 11} Ca^{2+} is unable to share ligands with Pb1 and
42 occupy the remaining vacant metal ion sites. The reason is high electronegativity of Pb^{2+} ³¹ that
43 results in protein-bound Pb1 depleting the electron density of the oxygen ligands³² shared by
44 Sites 1 and 2. It is therefore feasible that instead of Ca^{2+} , C2B·Pb1 will preferentially acquire
45 Pb^{2+} at Site 2, and that will drive the membrane association of Syt1 via the C2B domain. Our
46 results suggest that contribution of C2A to membrane binding in the chelating environment will
47
48
49
50
51
52
53
54
55
56
57
58
59
60

1
2
3 be significantly attenuated, because the C2A·Pb1 complex will neither engage with anionic
4 membranes nor bind Pb²⁺ at Site 2. Impaired membrane binding of the Ca²⁺-sensing region of
5 Syt1 could be a potential mechanism through which Pb²⁺ interferes with the regulation of Syt1
6 function by Ca²⁺ and disrupts the evoked release of neurotransmitters.³³⁻⁴⁰ By the same token,
7 Pb²⁺-driven partial membrane association of Syt1 could explain how Pb²⁺ induces sporadic
8 release of certain neurotransmitters.³⁷
9
10
11
12
13
14

15 CONCLUSION

16
17 Identification of oxygen-rich sites that Pb²⁺ could potentially target is essential for
18 understanding how Pb²⁺ interferes with the function of Ca²⁺-dependent signalling proteins.
19 Given low bioavailability of Pb²⁺, distinguishing and isolating high- from low-affinity protein
20 sites is essential. We demonstrated using two Ca²⁺-sensing C2 domains of Syt1, that Pb²⁺-
21 chelating pH buffer Bis-Tris provides the means to achieve such isolation. Pb²⁺ in Bis-Tris
22 populates only one site per C2 domain. The implication for Syt1 is that two of its Ca²⁺-binding
23 sites (out of total five) are likely to be targeted by Pb²⁺ in cellular milieu that contains natural
24 chelators. The effect of Bis-Tris on the metal-ion dependent membrane interactions of C2
25 domains revealed their differential response to Pb²⁺. Our results suggest that C2B rather than
26 C2A mediates the Pb²⁺-driven association of Syt1 with anionic membranes. Whether or not Pb²⁺
27 can displace Ca²⁺ from the membrane-bound C2 domains, isolated or in the context of full-length
28 Syt1, remains to be investigated. Our data on the C2 domain from PKC α ¹¹ suggest that at least
29 in the non-chelating environment Pb²⁺ can successfully displace Ca²⁺ from the protein in the
30 presence of anionic membranes.
31
32
33
34
35
36
37
38
39
40

41 Since protein-metal ion interactions are at the core of many biological processes,
42 extensive biochemical analysis of the corresponding binding equilibria is necessary. The use of
43 non-chelating pH buffers is intuitively preferred, to avoid possible complications presented by
44 metal ion chelation. This work provides a different perspective. If used in combination with
45 non-chelating buffers, chelating pH agents, such as Bis-Tris, could potentially provide valuable
46 mechanistic information that could otherwise be overlooked.
47
48
49
50
51
52
53
54
55
56
57
58
59
60

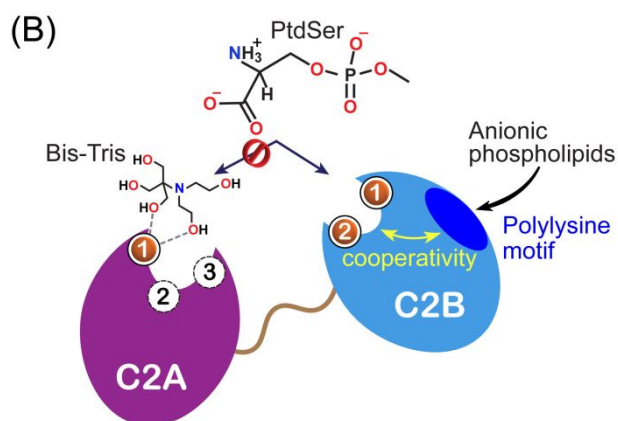
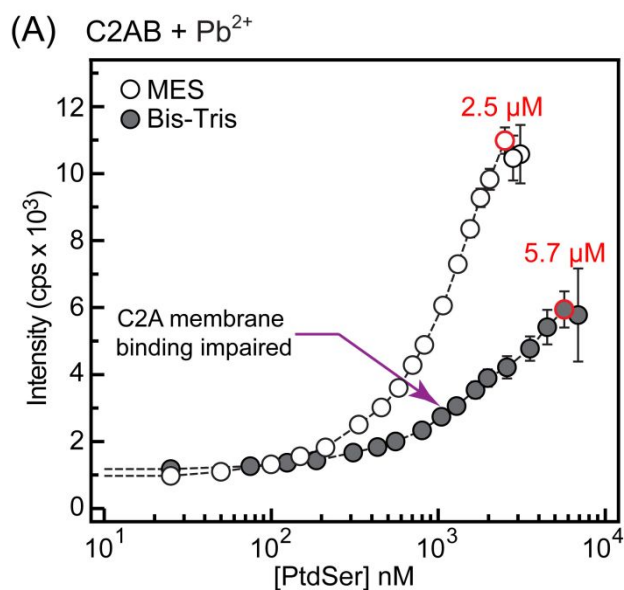


Figure 6. Membrane association of C2AB reflects the differential effect of Bis-Tris on the individual C2 domains. (A) C2AB-to-membrane binding curves plotted as a function of FRET efficiency versus concentration of accessible PtdSer in 100 nm LUVs. The concentration of C2AB and Pb²⁺ are 0.5 μM and 500 μM, respectively. The composition of LUVs is PtdSer:PtdCho:dansyl-PE=73:20:7 (molar). The buffer conditions are 20 mM Bis-Tris (MES) at pH 7.0 (6.0) with 150 mM KCl. The clustering point, at which light scattering by LUVs precludes further FRET measurements, is marked in red. More than 50% intensity difference in the dansyl-PE fluorescence intensity at the clustering point is observed in Bis-Tris compared to MES. (B) Schematic representation of the C2AB-Pb²⁺-anionic phospholipid interactions in the Bis-Tris environment. The association of anionic phospholipids with the polylysine cluster enables the population of Site 2 by Pb²⁺ and the coordination of protein-bound Pb²⁺ ions by PtdSer. Association of C2A with anionic membranes is extremely weak, because Bis-Tris interferes with Pb²⁺ binding to Sites 2 and 3, and PtdSer coordination by Pb²⁺.

Author Contributions: T.I.I. and S.K. designed the study. S.K. conducted the experiments and analyzed the data. T.I.I. and S.K. wrote the manuscript.

Acknowledgement: This work was supported in part by NSF CHE-1905116, NIH R01GM108998, and Welch A-1784, all to T.I.I.

REFERENCES

1. S. Caito, B. A. Lopes Ana Carolina, M. B. Paoliello Monica and M. Aschner, in *Lead – Its Effects on Environment and Health*, 2017, vol. 17.
2. T. I. Lidsky and J. S. Schneider, Lead neurotoxicity in children: basic mechanisms and clinical correlates, *Brain*, 2003, **126**, 5-19.
3. D. C. Bellinger, Very low lead exposures and children's neurodevelopment, *Current opinion in pediatrics*, 2008, **20**, 172-177.
4. R. Gorkhali, K. Huang, M. Kirberger and J. J. Yang, Defining potential roles of Pb²⁺ in neurotoxicity from a calciomics approach, *Metallomics*, 2016, **8**, 563-578.
5. M. Kirberger, H. C. Wong, J. Jiang and J. J. Yang, Metal toxicity and opportunistic binding of Pb²⁺ in proteins, *J. Inorg. Biochem.*, 2013, **125**, 40-49.
6. M. Geppert, Y. Goda, R. E. Hammer, C. Li, T. W. Rosahl, C. F. Stevens and T. C. Sudhof, Synaptotagmin I: a major Ca²⁺ sensor for transmitter release at a central synapse, *Cell*, 1994, **79**, 717-727.
7. C. M. Bouton, L. P. Frelin, C. E. Forde, H. Arnold Godwin and J. Pevsner, Synaptotagmin I is a molecular target for lead, *J. Neurochem.*, 2001, **76**, 1724-1735.
8. S. Katti, B. Her, A. K. Srivastava, A. B. Taylor, S. W. Lockless and T. I. Igumenova, High affinity interactions of Pb²⁺ with synaptotagmin I, *Metallomics*, 2018, **10**, 1211-1222.
9. K. H. Scheller, T. H. Abel, P. E. Polanyi, P. K. Wenk, B. E. Fischer and H. Sigel, Metal ion/buffer interactions. Stability of binary and ternary complexes containing 2-[bis(2-hydroxyethyl)amino]-2(hydroxymethyl)-1,3-propanediol (Bistris) and adenosine 5'-triphosphate (ATP), *Eur. J. Biochem.*, 1980, **107**, 455-466.
10. C. M. H. Ferreira, I. S. S. Pinto, E. V. Soares and H. M. V. M. Soares, (Un)suitability of the use of pH buffers in biological, biochemical and environmental studies and their interaction with metal ions – a review, *RSC Advances*, 2015, **5**, 30989-31003.
11. K. A. Morales, M. Lasagna, A. V. Gribenko, Y. Yoon, G. D. Reinhart, J. C. Lee, W. Cho, P. Li and T. I. Igumenova, Pb²⁺ as modulator of protein-membrane interactions, *J. Am. Chem. Soc.*, 2011, **133**, 10599-10611.
12. D. Long and D. Yang, Buffer interference with protein dynamics: a case study on human liver fatty acid binding protein, *Biophys. J.*, 2009, **96**, 1482-1488.
13. A. B. Seven, K. D. Brewer, L. Shi, Q. X. Jiang and J. Rizo, Prevalent mechanism of membrane bridging by synaptotagmin-1, *Proc. Natl. Acad. Sci. U. S. A.*, 2013, **110**, E3243-3252.
14. R. Fernandez-Chacon, A. Konigstorfer, S. H. Gerber, J. Garcia, M. F. Matos, C. F. Stevens, N. Brose, J. Rizo, C. Rosenmund and T. C. Sudhof, Synaptotagmin I functions as a calcium regulator of release probability, *Nature*, 2001, **410**, 41-49.

15. X. Zhang, J. Rizo and T. C. Sudhof, Mechanism of phospholipid binding by the C2A-domain of synaptotagmin I, *Biochemistry*, 1998, **37**, 12395-12403.
16. S. Katti, S. B. Nyenhuis, B. Her, D. S. Cafiso and T. I. Igumenova, Partial metal ion saturation of C2 domains primes Syt1-membrane interactions, *bioRxiv*, 2019, DOI: 10.1101/810010, 810010.
17. M. Hothorn, I. D'Angelo, J. A. Marquez, S. Greiner and K. Scheffzek, The invertase inhibitor Nt-CIF from tobacco: a highly thermostable four-helix bundle with an unusual N-terminal extension, *J. Mol. Biol.*, 2004, **335**, 987-995.
18. S. Y. Park, W. R. Lee, S. C. Lee, M. H. Kwon, Y. S. Kim and J. S. Kim, Crystal structure of single-domain VL of an anti-DNA binding antibody 3D8 scFv and its active site revealed by complex structures of a small molecule and metals, *Proteins*, 2008, **71**, 2091-2096.
19. H. T. Do, H. Li, G. Chreifi, T. L. Poulos and R. B. Silverman, Optimization of Blood-Brain Barrier Permeability with Potent and Selective Human Neuronal Nitric Oxide Synthase Inhibitors Having a 2-Aminopyridine Scaffold, *J. Med. Chem.*, 2019, **62**, 2690-2707.
20. J. A. Corbin, J. H. Evans, K. E. Landgraf and J. J. Falke, Mechanism of specific membrane targeting by C2 domains: localized pools of target lipids enhance Ca^{2+} affinity, *Biochemistry*, 2007, **46**, 4322-4336.
21. K. Duncan, Metallothioneins and Related Chelators. Metal Ions in Life Sciences Vol. 5., 2009, **48**, 7966-7967.
22. J. Bai, W. C. Tucker and E. R. Chapman, PIP_2 increases the speed of response of synaptotagmin and steers its membrane-penetration activity toward the plasma membrane, *Nat. Struct. Mol. Biol.*, 2004, **11**, 36-44.
23. A. Perez-Lara, A. Thapa, S. B. Nyenhuis, D. A. Nyenhuis, P. Halder, M. Tietzel, K. Tittmann, D. S. Cafiso and R. Jahn, PtdInsP₂ and PtdSer cooperate to trap synaptotagmin-1 to the plasma membrane in the presence of calcium, *Elife*, 2016, **5**.
24. M. Xue, C. Ma, T. K. Craig, C. Rosenmund and J. Rizo, The Janus-faced nature of the C₂B domain is fundamental for synaptotagmin-1 function, *Nat. Struct. Mol. Biol.*, 2008, **15**, 1160-1168.
25. G. van den Bogaart, K. Meyenberg, U. Diederichsen and R. Jahn, Phosphatidylinositol 4,5-bisphosphate increases Ca^{2+} affinity of synaptotagmin-1 by 40-fold, *J. Biol. Chem.*, 2012, **287**, 16447-16453.
26. S. Katti, S. B. Nyenhuis, B. Her, A. K. Srivastava, A. B. Taylor, P. J. Hart, D. S. Cafiso and T. I. Igumenova, Non-Native Metal Ion Reveals the Role of Electrostatics in Synaptotagmin 1-Membrane Interactions, *Biochemistry*, 2017, **56**, 3283-3295.
27. M. S. Perin, N. Brose, R. Jahn and T. C. Sudhof, Domain structure of synaptotagmin (p65), *J. Biol. Chem.*, 1991, **266**, 623-629.
28. D. Arac, X. Chen, H. A. Khant, J. Ubach, S. J. Ludtke, M. Kikkawa, A. E. Johnson, W. Chiu, T. C. Sudhof and J. Rizo, Close membrane-membrane proximity induced by Ca^{2+} -dependent multivalent binding of synaptotagmin-1 to phospholipids, *Nat. Struct. Mol. Biol.*, 2006, **13**, 209-217.
29. D. Z. Herrick, W. Kuo, H. Huang, C. D. Schwieters, J. F. Ellena and D. S. Cafiso, Solution and membrane-bound conformations of the tandem C2A and C2B domains of synaptotagmin 1: Evidence for bilayer bridging, *J. Mol. Biol.*, 2009, **390**, 913-923.
30. M. Ahamed and M. K. Siddiqui, Low level lead exposure and oxidative stress: current opinions, *Clin. Chim. Acta*, 2007, **383**, 57-64.

- 1
2
3 31. W. Gordy and W. J. O. Thomas, Electronegativities of the Elements, 1956, **24**, 439-444.
4 32. T. Dudev, C. Grauffel and C. Lim, How Pb²⁺ Binds and Modulates Properties of Ca²⁺-
5 Signaling Proteins, *Inorg. Chem.*, 2018, **57**, 14798-14809.
6 33. R. S. Manalis and G. P. Cooper, Letter: Presynaptic and postsynaptic effects of lead at the
7 frog neuromuscular junction, *Nature*, 1973, **243**, 354-356.
8 34. P. T. Carroll, E. K. Silbergeld and A. M. Goldberg, Alteration of central cholinergic
9 function by chronic lead acetate exposure, *Biochem. Pharmacol.*, 1977, **26**, 397-402.
10 35. D. J. Minnema, R. D. Greenland and I. A. Michaelson, Effect of in vitro inorganic lead on
11 dopamine release from superfused rat striatal synaptosomes, *Toxicol. Appl. Pharmacol.*,
12 1986, **84**, 400-411.
13 36. D. J. Minnema, I. A. Michaelson and G. P. Cooper, Calcium efflux and neurotransmitter
14 release from rat hippocampal synaptosomes exposed to lead, *Toxicol. Appl. Pharmacol.*,
15 1988, **92**, 351-357.
16 37. L. Struzynska and U. Rafalowska, The effect of lead on dopamine, GABA and histidine
17 spontaneous and KCl-dependent releases from rat brain synaptosomes, *Acta Neurobiol.*
18 *Exp.*, 1994, **54**, 201-207.
19 38. S. M. Lasley and M. E. Gilbert, Presynaptic glutamatergic function in dentate gyrus in vivo
20 is diminished by chronic exposure to inorganic lead, *Brain Res.*, 1996, **736**, 125-134.
21 39. M. T. Antonio and M. L. Leret, Study of the neurochemical alterations produced in discrete
22 brain areas by perinatal low-level lead exposure, *Life Sci.*, 2000, **67**, 635-642.
23 40. S. M. Lasley and M. E. Gilbert, Rat hippocampal glutamate and GABA release exhibit
24 biphasic effects as a function of chronic lead exposure level, *Toxicol. Sci.*, 2002, **66**, 139-
25 147.
26
27
28
29
30
31
32
33
34
35
36
37
38
39
40
41
42
43
44
45
46
47
48
49
50
51
52
53
54
55
56
57
58
59
60